Original Scientific Article • DOI: 10.2478/rmzmag-2023-0001

Received: January 23, 2023
Accepted: February 14, 2023

Mineral Chemistry of Pyroxene Gneiss in Obudu, SE Nigeria, and Its Petrological Significance

Mineralna kemija piroksenitnega gnajsa iz Obuduja, JV Nigerija in njegov petrološki pomen

Ifeoma Agbi[1,*], Emmanuel M. Iroka[2]

[1]Department of Physics/Geology/Geophysics, Alex Ekwueme Federal University Ndufu-Alike, Ebonyi State, Nigeria

[2]Department of Geology, University of Calabar, Calabar, Cross River, Nigeria

*Corresponding author: E-mail: ifya@rocketmail.com

Abstract

The pyroxene gneiss which forms part of the basement cover in southeast Nigeria is a coarse-grained weakly foliated rock that has experienced high-grade metamorphism and anatexis. Electron microprobe data obtained from samples of this pyroxene-bearing gneiss confirm that the essential minerals are plagioclase (andesine, $An_{30 - 37}$), orthopyroxene (hypersthene, $En_{55.3 - 61.2}$, $Wo_{1.0 - 2.6}$, $Fs_{36.3 - 43.7}$), and clinopyroxene (augite, $En_{39.7 - 42.3}$, $Wo_{42.0 - 45.1}$, $Fs_{14.2 - 17.0}$). This assemblage is a typical granulite facies mineralogy produced by igneous rocks with intermediate to mafic composition that have been metamorphosed at medium pressure. Other minerals are calcic amphibole (X_{Mg} = 0.56–0.59), biotite (X_{Mg} = 0.58–0.69), orthoclase, and quartz. Orthoclase occurs mainly in leucocratic bands and clinopyroxene absent samples and may have resulted from dehydration reaction and thus dissolved in the melt phase. Fe -Ti oxides of ilmenite, hematite, and magnetite occur as accessory minerals, giving the imprint of metamorphism under oxidizing conditions. The presence of exsolved titanohematite in ilmenite indicates retrogressive metamorphism.

Keywords: mineral chemistry, pyroxene gneiss, electron microprobe, Obudu

Povzetek

Piroksenitni gnajs, ki tvori del bazalnega kompleksa v JV Nigeriji je debelozrnata kamnina s slabo izraženo foliacijo, ki je prešla visoko stopnjo metamorfizma in anatekse. Preiskave z elektronsko mikrosondo potrjujejo, da so bistveni minerali v kamnini plagioklaz (andezin, $An_{30 - 37}$), ortopiroksen (hipersten, $En_{55.3 - 61.2}$, $Wo_{1.0 - 2.6}$, $Fs_{36.3 - 43.7}$) in klinopiroksen (avgit, augite, $En_{39.7 - 42.3}$, $Wo_{42.0 - 45.1}$, $Fs_{14.2 - 17.0}$). Ta združba je značilna mineralogija granulitnega faciesa, nastalega iz magmatskih kamnin srednje do mafične sestave, ki so bile metamorfozirane pri zmerno močnem pritisku. Drugi minerali so kalcijev amfibol (X_{Mg} = 0.56–0.59), biotit (X_{Mg} = 0.58–0.69), ortoklaz in kremen. Ortoklaz se večinoma pojavlja v levkokratnih pasovih ter v vzorcih brez klinopiroksena in je morda nastal z dehidratacijo ter se kot tak v fazi taline raztopil. Kot akcesorni minerali se pojavljajo Fe-Ti oksidi ilmenita, hematita in magnetita, ki kažejo na metamorfizem v oksidativnih razmerah. Izločanje titanohematita v ilmenitu je retrogradna metamorfna sprememba.

Ključne besede: mineralna kemija, piroksenitni gnajs, elektronska mikrosonda, Obudu

Introduction

The Benin–Nigeria Shield exposed in Nigeria comprises rocks that are commonly grouped into the Migmatite Gneiss Complex, Schist Belts, and Pan-African granitoids [1–3]. The pyroxene gneiss which forms part of the basement cover in southeast Nigeria belongs to the Migmatite Gneiss Complex and has a reported age of 2062.4 ± 0.4 Ma from single zircon evaporation method [4]. These rocks outcrop in places such as the Okorotong, Bebi, Bogene, and Abado areas of Obudu (Figure 1). Lithologically, the rocks are mesocratic and coarse-grained with minor leucocratic bands appearing in some places. Ekwueme and Kröner [4] suggested the pyroxene gneiss may have originated from a metagreywacke or granodiorite protolith; Ugwuonah et al. [5], however, termed the rock a meta quartz diorite. The rocks have experienced high-grade metamorphism up to granulite facies [4–6]. This work aims to study the mineral chemistry obtained from an electron microprobe analyzer (EMPA) in order to distinguish the different mineral phases and thus infer their petrological significance.

Geological setting

The pyroxene gneiss which outcrops at Obudu is one of the rock types in the area (Figure 1). Other rocks occurring in the area include migmatite gneisses, granitic gneisses, amphibolites, and meta-ultramafics which have subsequently been intruded by granitoids and other unmetamorphosed rocks. These rocks, which form part of the basement cover in southeast Nigeria, have experienced at least three episodes of deformation [7]. Some of the rocks have been dated with ages of Paleoproterozoic, Neoproterozoic, and Pan African [4, 8]. The Nigerian basement complex is part of the Trans Sahara Orogenic belt and is situated within the reactivated region resulting from the collision of the West African craton and the Congo craton [3].

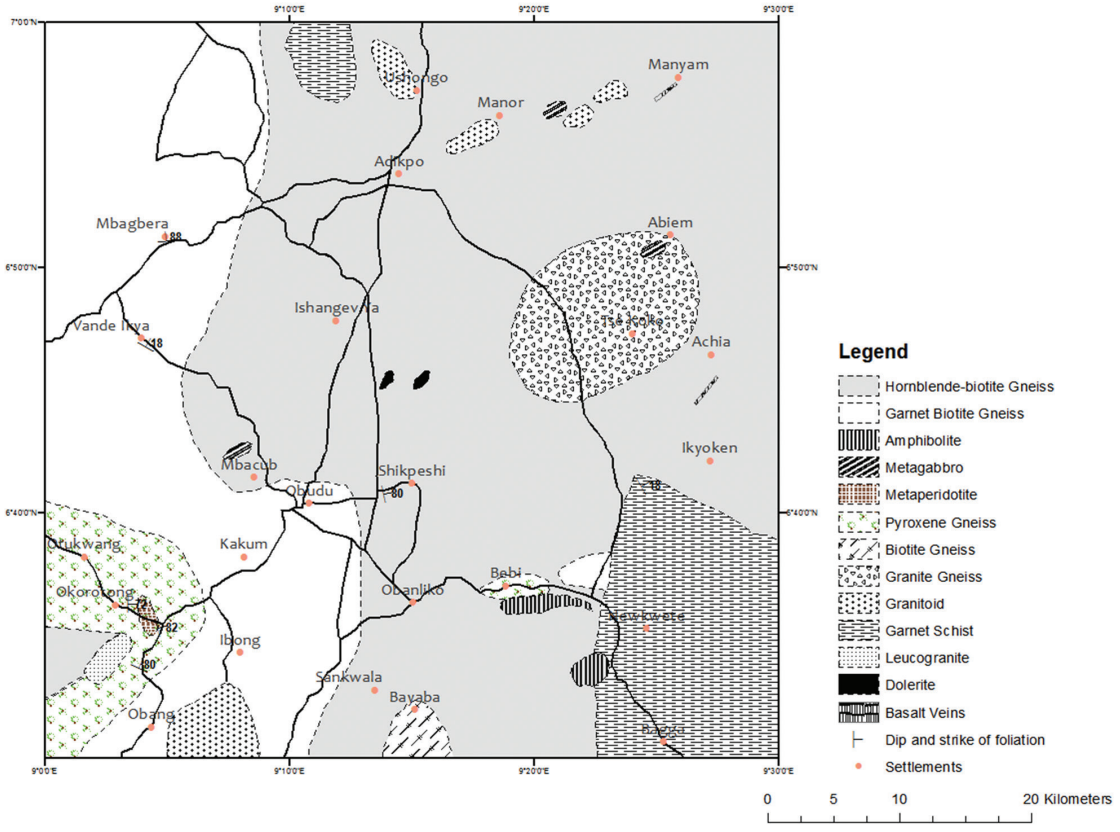

Figure 1: *Geologic map of Obudu Plateau.*

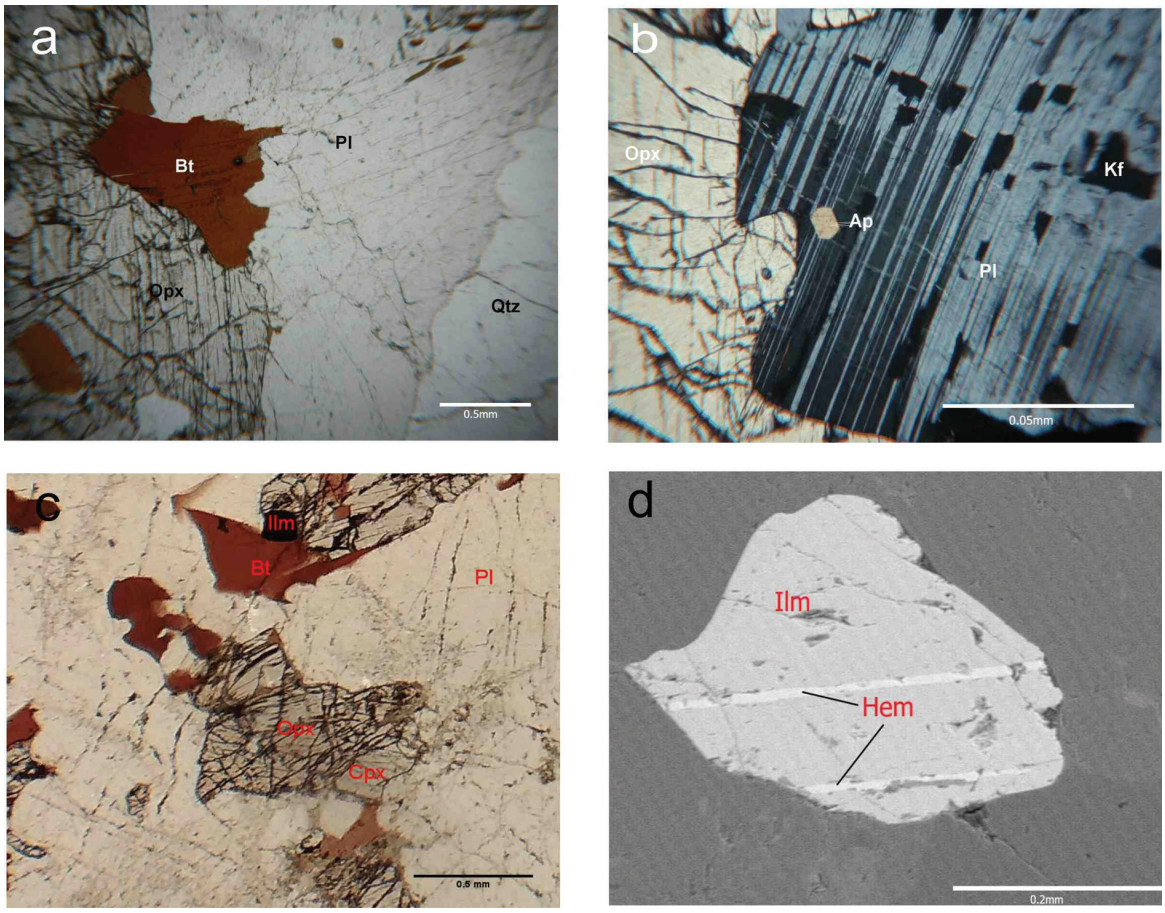

Figure 2: *Photomicrograph of pyroxene gneiss showing (a) mineral association of orthopyroxene + plagioclase+ biotite + quartz in sample IA5 (PPL); (b) Antiperthite texture in plagioclase of IA5 and apatite inclusion (XPL); (c) Mineral assemblage in sample IA3 showing clinopyroxene occurring alongside orthopyroxene (PPL); (d) BSE image of exsolved laths of hematite in ilmenite in sample IA3.*

Materials and methods

The petrography of samples collected from the pyroxene gneiss was ascertained using a petrographic microscope at the Department of Geology, University of Calabar. Electron microprobe analyses were subsequently performed on two polished samples using a CAMECA SX FIVE FE at Ruhr Universität, Bochum, Germany. Analyses were performed using LTAP, TAP, LPET, PET, and LLIF crystals on five wavelength dispersive spectrometers at 15KV accelerating voltage, 15nA beam current, and 5µm probe diameter. Ten elements (Si, Al, Fe, Ca, Na, K, Ti, Cr, Mn, Mg) were quantitatively analyzed using natural and synthetic minerals as standards. The concentrations were calculated using the PAP matrix correction factors.

Results and discussion

Petrography

These rocks are weakly foliated, and, in some locations, metamorphic segregation is observed as irregular banding. One of the thin sections (IA5) was cut through a leucosome band. In terms of texture, the rocks are coarse-grained and exhibit deformation structures such as fractures, pinch and swell structures, and augens. Mineralogically, the rock contains the assemblage plagioclase + orthopyroxene + clinopyroxene + biotite + quartz ± k-feldspar ± amphibole. Accessory phases include ilmenite, magnetite, apatite, pyrite, and zircons. A slight alignment of minerals is observed under the microscope. Plagioclase is the dominant mineral in the matrix (40%–50% vol) and contains

Table 1: *Representative chemical composition (wt%) and atom per formula unit of plagioclase based on 8 oxygen. (sample IA3/5).*

Sample	IA3					IA5				
Wt%	**1**	**2**	**3**	**4**	**5**	**1**	**2**	**3**	**4**	**5**
SiO_2	60.55	60.58	60.57	60.48	60.44	60.13	60.07	60.20	59.91	60.95
Al_2O_3	25.33	25.02	25.12	25.43	25.55	25.75	25.18	25.17	25.49	24.90
FeO*	0.09	0.09	0.11	0.10	0.11	0.02	0.05	0.05	0.10	0.07
CaO	6.31	6.48	6.67	6.36	6.55	6.82	6.75	6.72	6.91	6.24
Na_2O	7.40	7.67	7.47	7.49	7.65	7.45	7.32	7.43	7.41	7.66
K_2O	0.68	0.50	0.40	0.55	0.43	0.35	0.53	0.62	0.39	0.46
Total	100.36	100.34	100.35	100.41	100.73	100.52	99.90	100.19	100.20	100.29
apfu										
Si	2.692	2.690	2.694	2.686	2.673	2.668	2.684	2.681	2.667	2.709
Al	1.327	1.309	1.317	1.331	1.332	1.347	1.326	1.321	1.337	1.304
Fe^{3+}	0.000	0.000	0.000	0.000	0.001	0.000	0.000	0.000	0.000	0.000
Fe^{2+}	0.003	0.003	0.004	0.004	0.003	0.001	0.002	0.002	0.004	0.003
Ca	0.301	0.308	0.318	0.303	0.310	0.324	0.323	0.320	0.330	0.297
Na	0.638	0.661	0.644	0.645	0.656	0.641	0.634	0.641	0.640	0.660
K	0.038	0.028	0.023	0.031	0.024	0.020	0.030	0.035	0.022	0.026
Total	5.000	5.000	5.000	5.000	5.000	5.000	5.000	5.000	5.000	5.000
End Member Fractions (mol%)										
An	30.77	30.91	32.26	30.93	31.33	32.92	32.72	32.15	33.26	30.21
Ab	65.30	66.27	65.43	65.91	66.21	65.09	64.23	64.33	64.51	67.12
Or	3.93	2.82	2.31	3.16	2.46	1.99	3.06	3.52	2.23	2.67

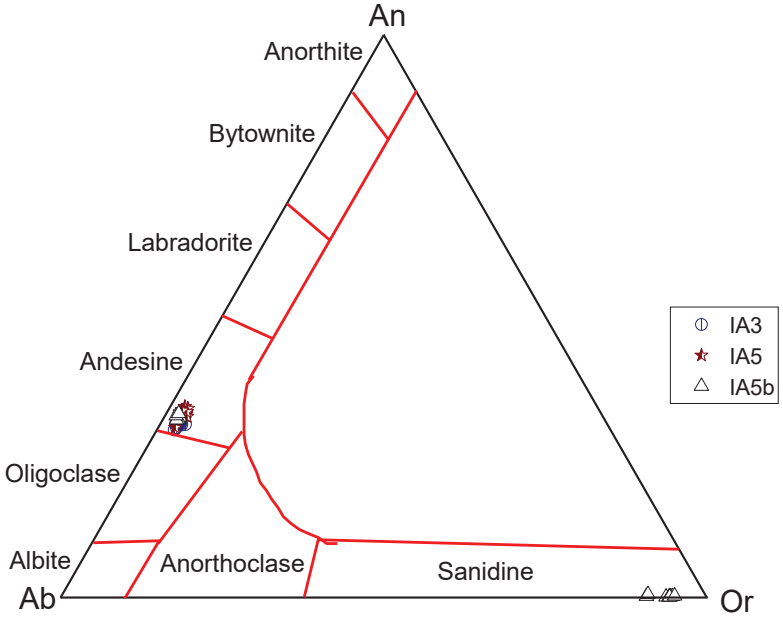

Figure 3: *An-Ab-Or plot for the pyroxene gneiss of Obudu showing andesine as the main plagioclase.*

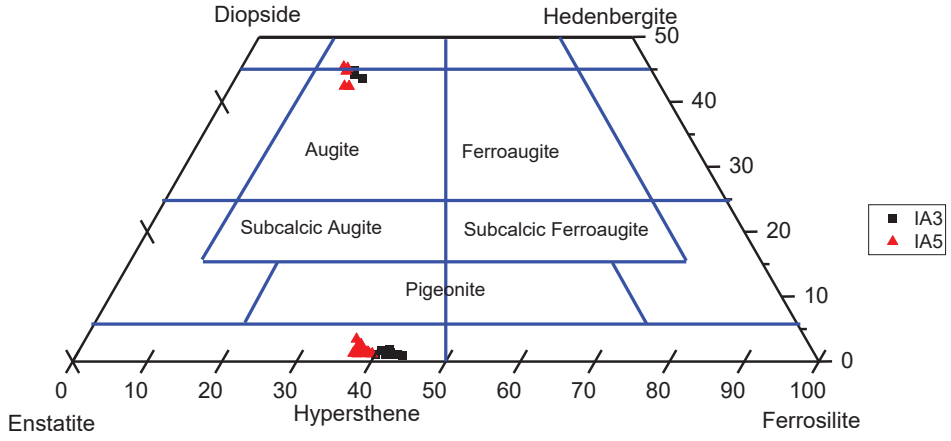

Figure 4: *Pyroxene triangular diagram showing the occurrence of hypersthene and augite in the pyroxene gneiss.*

Table 2: *Representative chemical composition (wt%) and atom per formula unit (apfu) of orthopyroxene based on 6 oxygen. (sample IA3/5).*

Sample	**IA3**					**IA5**				
Wt%	**1**	**2**	**3**	**4**	**5**	**1**	**2**	**3**	**4**	**5**
SiO_2	51.68	51.86	52.20	52.05	52.20	52.94	52.82	52.87	52.98	52.98
TiO_2	0.10	0.09	0.05	0.11	0.09	0.08	0.10	0.09	0.08	0.10
Al_2O_3	0.87	0.85	0.92	0.77	0.80	0.49	0.58	0.53	0.57	0.64
Cr_2O_3	0.02	0.01	0.00	0.03	0.00	0.05	0.10	0.05	0.05	0.08
FeO*	25.46	25.42	24.74	25.07	26.72	24.49	22.65	23.40	23.30	23.15
MnO	0.66	0.64	0.61	0.64	0.76	0.69	0.61	0.63	0.61	0.59
MgO	19.69	19.83	20.38	20.03	18.94	20.89	21.07	21.49	21.23	21.35
CaO	0.82	0.64	0.51	0.80	0.46	0.57	1.69	0.73	0.85	1.04
Na_2O	0.00	0.02	0.01	0.03	0.01	0.00	0.05	0.00	0.04	0.04
K_2O	0.00	0.01	0.00	0.00	0.01	0.03	0.01	0.00	0.01	0.00
Total	99.32	99.37	99.43	99.54	99.99	100.23	99.67	99.80	99.72	99.99
apfu										
Si	1.971	1.975	1.979	1.976	1.990	1.989	1.985	1.985	1.992	1.985
Ti	0.003	0.003	0.002	0.003	0.003	0.002	0.003	0.002	0.002	0.003
Al	0.039	0.038	0.041	0.035	0.036	0.022	0.026	0.024	0.025	0.028
Cr	0.001	0.000	0.000	0.001	0.000	0.001	0.003	0.001	0.001	0.003
Fe^{3+}	0.013	0.007	0.000	0.008	0.000	0.000	0.000	0.000	0.000	0.000
Fe^{2+}	0.799	0.802	0.785	0.788	0.852	0.770	0.712	0.735	0.733	0.725
Mn	0.021	0.021	0.020	0.020	0.025	0.022	0.019	0.020	0.020	0.019
Mg	1.119	1.126	1.152	1.134	1.076	1.170	1.181	1.203	1.190	1.192
Ca	0.033	0.026	0.021	0.033	0.019	0.023	0.068	0.029	0.034	0.042
Na	0.000	0.001	0.001	0.002	0.001	0.000	0.004	0.000	0.003	0.003
Total	4.000	4.000	4.000	4.000	4.000	4.000	4.000	4.000	4.000	4.000
X_{Mg}	0.58	0.58	0.59	0.59	0.56	0.60	0.62	0.62	0.62	0.62
End Member Fractions(%)										
Wo	1.70	1.32	1.07	1.67	0.97	1.18	3.47	1.50	1.76	2.13
En	56.98	57.40	58.85	57.77	55.28	59.61	60.22	61.15	60.80	60.85
Fs	41.32	41.28	40.08	40.57	43.75	39.22	36.31	37.36	37.44	37.02

Table 3: *Representative chemical composition (wt%) and atom per formula unit (apfu) of calcic amphibole and clinopyroxene based on 23 oxygen and 6 oxygen, respectively. (sample IA3/5)*

Amphibole						**Clinopyroxene**			
Sample	**IA3**					**IA3**		**IA5**	
Wt%	**1**	**2**	**3**	**4**	**5**	**1**	**2**	**1**	**2**
SiO_2	42.71	42.70	42.86	41.79	43.34	52.67	52.74	53.24	52.89
TiO_2	2.59	2.39	2.06	2.49	2.48	0.16	0.13	0.07	0.16
Al_2O_3	11.11	10.57	10.77	11.40	10.51	1.49	1.39	1.44	1.50
Cr_2O_3	0.13	0.05	0.06	0.10	0.08	0.00	0.02	0.08	0.08
FeO*	14.09	15.61	15.77	15.84	15.30	9.41	10.37	9.66	9.17
MnO	0.11	0.15	0.15	0.16	0.15	0.31	0.30	0.31	0.32
MgO	11.58	11.30	11.01	10.55	11.46	13.66	13.42	14.27	14.30
CaO	11.42	11.18	11.51	11.48	11.29	21.48	20.74	20.17	19.95
Na_2O	1.35	1.53	1.01	1.22	1.35	0.41	0.48	0.36	0.41
K_2O	1.61	1.37	1.43	1.55	1.33	0.00	0.00	0.00	0.00
Total	96.70	96.86	96.63	96.58	97.29	99.59	99.58	99.60	98.76
apfu									
Si	6.382	6.379	6.414	6.296	6.427	1.972	1.980	1.991	1.991
Ti	0.291	0.269	0.231	0.282	0.277	0.004	0.004	0.002	0.004
Al	1.956	1.861	1.900	2.024	1.836	0.066	0.062	0.063	0.066
Cr	0.016	0.005	0.007	0.011	0.010	0.000	0.000	0.002	0.002
fe3	0.326	0.555	0.548	0.448	0.518	0.012	0.006	0.000	0.000
Fe^{2+}	1.435	1.394	1.426	1.548	1.379	0.283	0.319	0.302	0.289
Mn	0.013	0.019	0.019	0.020	0.019	0.010	0.009	0.010	0.010
Mg	2.581	2.517	2.456	2.371	2.534	0.762	0.751	0.796	0.802
Ca	1.829	1.790	1.845	1.854	1.794	0.861	0.834	0.808	0.804
Na	0.391	0.442	0.293	0.356	0.390	0.030	0.035	0.026	0.030
K	0.306	0.262	0.273	0.297	0.251				
Total	15.527	15.493	15.411	15.506	15.434	4.000	4.000	4.000	4.000
X_{Mg}	0.59	0.56	0.55	0.54	0.57	0.72	0.70	0.72	0.74
End Member Fractions(mol%)									
Wo						44.90	43.66	42.40	42.44
En						39.74	39.31	41.75	42.33
Fs						15.36	17.03	15.85	15.22

inclusions of quartz and apatite. K-feldspar is only present in the leucosome, where it is associated with plagioclase, quartz, and orthopyroxene. Hematite occurs as exsolved laths in ilmenite (Figure 2).

Mineral chemistry

Feldspar

The sodic plagioclase andesine (An_{30} to An_{37}) with less than 4% orthoclase content occurs in the pyroxene gneiss. In the leucocratic band where antiperthite occurs, the exsolved laths are orthoclase-rich (Or_{93-95}, Ab_{4-6}, $An_{0.1-0.4}$) and occur within sodic-rich plagioclase of similar composition (An_{35}) as the matrix plagioclase.

K-feldspar, where it occurred, had a similar composition to the exsolved laths in the antiperthite (Or_{91}, Ab_{9}, $An_{0.3}$). (Table 1, Figure 3).

Orthopyroxene

The orthopyroxene is hypersthene, as seen in Figure 4 and Table 2. X_{Mg} = 0.56–0.62.

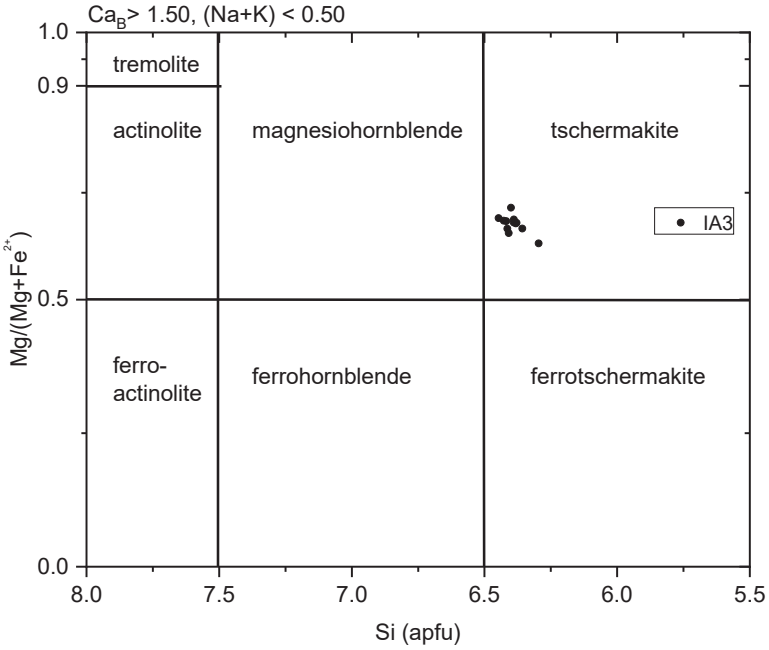

Figure 5: *Si Vs Mg/(Mg +Fe^{2+}) diagram for amphiboles from sample IA3 shown as tschermakite.*

Clinopyroxene

The clinopyroxene is also magnesium-rich (X_{Mg} = 0.70–0.74). In terms of wollastonite, enstatite, and ferrosilite, the range is Wo_{42-45}, En_{39-42}, Fs_{14-17}. It plots in the field of augite (Figure 4, Table 3).

Calcic–Amphibole

The calcic amphibole occupies about 1% volume in the studied samples and can be classified as tschermakite according to the classification scheme of Leake et al. [9]. X_{Mg} = 0.56–0.59 (Figure 5).

Biotite

The biotite in the samples is Mg-rich (X_{Mg} = 0.58–0.69) and has Ti content of 0.5–0.6 p.f.u. for both samples. Matrix X_{Mg} values are lower than values for biotite adjacent to orthopyroxene (Table 4).

Other minerals

The TiO_2 content of the ilmenite in this rock varies from 41.9 wt% to 49.9 wt%, while the FeO content of the ilmenite varies from 46.99 wt% to 52.96 wt%. Hematite microprobe data yields 89.64 wt% to 90.36 wt% FeO with about 1.79 wt% TiO_2 occurring in the exsolved lamella. In contrast, magnetite had a FeO content of 92.60 wt%.

Petrological significance

Rocks of intermediate to mafic composition, such as andesite, diorite, basalt, and gabbro, when metamorphosed at high metamorphic grade, are usually marked by the appearance of certain minerals. The appearance of orthopyroxene in a rock with typical metabasite composition defines the onset of granulite facies metamorphism. The typical assemblage of such rocks at granulite facies include orthopyroxene + clinopyroxene + plagioclase ± hornblende ± garnet ± biotite ± quartz ± rutile ± ilmenite [10]. At higher pressures above 7 kbar, the distinctive assemblage is plagioclase + augite + garnet, while at lower pressures between 5–7 kbar, the typical assemblage is plagioclase + augite + hypersthene [11].

During the transition from the amphibolite to the granulite facies, hydrous phases such as amphibole decrease in modal amount with increasing temperature, by the reaction:

Hornblende + quartz = orthopyroxene + clinopyroxene + plagioclase + H_2O(1)[10]

Table 4: *Representative chemical composition (wt%) and atom per formula unit (apfu) of biotite based on 22 oxygen (sample IA3/5).*

Sample	IA3				IA5				
Remarks	**Core adjacent Opx**	**Rim adjacent Opx**	**Matrix 1**	**Matrix 2**	**Inclusion**	**Rim adjacent Opx**	**Core adjacent Opx**	**Matrix 1**	**Matrix 2**
SiO_2	36.65	36.42	35.82	35.79	37.68	38.06	37.54	37.34	37.29
TiO_2	5.05	4.80	5.18	5.07	5.54	5.27	5.15	5.80	5.88
Al_2O_3	14.87	13.94	13.99	14.03	14.18	14.39	14.36	14.23	13.87
Cr_2O_3	0.04	0.04	0.05	0.07	0.45	0.44	0.40	0.44	0.41
FeO*	14.65	16.62	16.40	16.81	12.74	12.19	13.12	13.69	13.67
MnO	0.01	0.09	0.11	0.06	0.03	0.05	0.04	0.07	0.04
MgO	13.81	13.23	12.27	12.66	14.80	15.45	15.12	14.26	14.04
CaO	0.00	0.00	0.02	0.00	0.07	0.00	0.01	0.07	0.00
Na_2O	0.03	0.03	0.03	0.04	0.11	0.05	0.05	0.11	0.04
K_2O	9.37	9.34	9.42	9.34	9.50	9.64	9.67	9.41	9.63
Total	94.49	94.51	93.28	93.86	95.09	95.53	95.47	95.41	94.87
apfu									
Si	5.519	5.547	5.535	5.504	5.591	5.601	5.563	5.550	5.580
Ti	0.572	0.550	0.602	0.586	0.618	0.584	0.574	0.648	0.661
Al	2.640	2.504	2.548	2.543	2.480	2.497	2.509	2.493	2.447
Cr	0.005	0.005	0.006	0.009	0.053	0.052	0.047	0.052	0.049
Fe^{2+}	1.845	2.117	2.119	2.162	1.581	1.500	1.626	1.702	1.711
Mn	0.002	0.011	0.014	0.008	0.003	0.006	0.005	0.008	0.005
Mg	3.099	3.003	2.825	2.901	3.273	3.388	3.338	3.159	3.132
Ca	0.000	0.000	0.003	0.000	0.011	0.000	0.001	0.011	0.000
Na	0.009	0.007	0.009	0.013	0.031	0.013	0.015	0.031	0.012
K	1.800	1.816	1.857	1.832	1.799	1.810	1.828	1.783	1.839
Total	15.491	15.560	15.519	15.557	15.439	15.452	15.507	15.437	15.436
X_{Mg}	0.63	0.59	0.57	0.57	0.67	0.69	0.67	0.65	0.65

As observed in the pyroxene gneiss, hornblende is completely absent from sample IA5 and is only about 1% vol in sample IA3. Also, the orthopyroxene and plagioclase occupy more than 60% volume of the rock. This suggests that pyroxene gneiss had attained granulite facies metamorphism.

At the beginning of granulite facies metamorphism, during anatexis, orthoclase is formed by the reaction:

$$\text{Biotite + quartz = orthopyroxene + orthoclase + } H_2O \text{ (2) [11]}$$

The orthoclase and orthopyroxene produced from the dehydration reaction of biotite will enter into the melt phase and be preserved in the rock as leucocratic quartzofeldspathic bands called leucosomes. This explains the presence of orthoclase only in the leucocratic bands of IA5, where it is associated with orthopyroxene and minor biotite. Anhydrous mafic granulites form at temperatures above 850 °C, but in the presence of water-rich fluids, mafic rocks can undergo partial melting and granulites will form at temperatures below 750 °C [11]. Geothermometric calculations based on hornblende and plagioclase geothermometer by Holland and Blundy [12] gave temperatures of 690–740 °C at 5.2 kbar [5]. Although these low values fall within the temperature and pressure values for migmatitic pyroxene granulites, it has been interpreted as post-peak reequilibration. The exsolution of ilmenite to ilmenite + titanohematite (Figure 2d) occurs due to slow cooling or retrogressive metamorphism [13] and is a further indication of retrogressive metamorphism.

Conclusions

The pyroxene gneiss has the mineralogic assemblage of plagioclase + clinopyroxene + orthopyroxene characteristic of metabasites that attained granulite facies metamorphism at pressures below 7 kbar. The presence of migmatitic structures attests to the presence of H_2O-rich fluids during metamorphism and ensuing lower peak metamorphic temperature. Mineral chemistry data shows that the rock is Mg-rich, as X_{Mg} values vary from 0.54–0.74 across the Fe-Mg minerals.

Acknowledgements

The authors are indebted to Prof. Sumit Chakraborty of the Institute of Geology, Mineralogy and Geophysics at the Ruhr University, Bochum, Germany for accepting IA as a guest researcher at the institute and for use of EMPA.

References

[1] Rahaman, M.A. (1988): Recent advances in the study of the basement complex of Nigeria. In: *Precambrian Geology of Nigeria*, Oluyide, P.O. (ed). Geological Survey of Nigeria Publication: Nigeria, pp. 11–43.

[2] Ekwueme, B.N. (2003): *The Precambrian geology and evolution of southeastern Nigerian Basement Complex*. University of Calabar Press: Calabar, 135 p.

[3] Dada, S.S. (2008): Proterozoic evolution of the Nigeria – Boborema province. In: *West Gondwana: Pre-Cenozoic correlations across the South Atlantic region*. Geological Society Special Publication: London, pp.121–136, DOI: 10.1144/SP294.7.

[4] Ekwueme, B.N., Kröner, A. (2006): Single zircon ages of migmatitic gneisses and granulites in the Obudu Plateau: Timing of granulite-facies metamorphism in southeastern Nigeria. *Journal of African Earth Sciences,* 44 pp. 459–469, DOI: 10.1016/j.jafrearsci.2005.11.013.

[5] Ugwuonah, E.N., Tsunogae, T., Ekwueme, B.N. (2019): Petrology and phase equilibrium modelling of granulites from Obudu in the Benin-Nigerian Shield, Southeastern Nigeria: Implications for clockwise P-T evolution in a collisional orogen. *Mineralogy and Petrology,* 113(3), pp. 353–368, DOI: 10.1007/s00710-019-00652-4.

[6] Ukwang, E.E., Ekwueme, B.N., Horsley, R.J. (2003): Petrology of granulite facies rocks in Ukwortung area of Obudu Plateau, Southeastern Nigeria. *Global Journal of Geological Sciences*, 1(2), pp. 159–167.

[7] Dada, S.S. (1998): Crust-forming ages and proterozoic crustal evoluton in Nigeria: a reappraisal of current interpretations. *Precambrian Research,* 87(1–2), pp. 65–74, DOI: 10.1016/S0301-9268(97)00054-5.

[8] Ukwang, E.E., Ekwueme, B.N., Kröner, A. (2012): Single zircon evaporation ages: Evidence for

the Mesoproterozoic crust in the southeastern Nigerian basement complex. *Chinese Journal of Geochemistry,* 31(1), pp. 48–54, DOI: 10.1007/s11631-012-0548-4.

[9] Leake, B., Woolley, A., Arps, C., Birch, W., Gilbert, M., Grice, J., Hawthrone, F., Kato, A., Kisch, H., Krivovichev, V., Linthout, K., Laird, J., Mandarino, J., Maresch, W., Nickel, E., Rock, N., Schumacher, J., Smith, D., Stephenson, N., Ungaretti, L., Whittaker, E., Youzhi, G. (1997): Nomenclature of amphiboles: Report of the subcommittee on amphiboles of the International Mineralogical Association, commission on new minerals and mineral names. *The Canadian Mineralogist*, 35(1), 219–246.

[10] Spear, F.S. (1993): *Metamorphic Phase Equilibria and Pressure-Temperature-Time Paths.* Mineralogical Society of America: Washington, D.C, 799 p.

[11] Bucher, K., Grapes R. (2011): *Petrogenesis of Metamorphic Rocks*. Springer: Berlin, Heidelberg, 428 p.

[12] Holland, T., Blundy, J. (1994): Non-ideal interactions in calcic amphiboles and their bearing on amphibole-plagioclase thermometry. *Contributions to Mineralogy and Petrology*, 116(4), 433–447, DOI: 10.1007/BF00310910.

[13] Frost, B.R. (1991): Stability of oxide minerals in metamorphic rocks. In: *Oxide Minerals: Petrologic and Magnetic Significance,* Lindsley, D.H. (ed). DeGruyter: Berlin, pp. 469–488.